

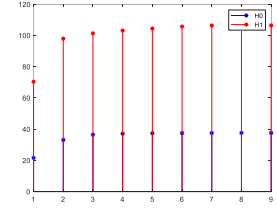
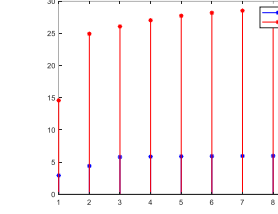
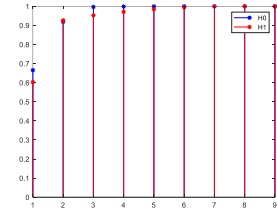
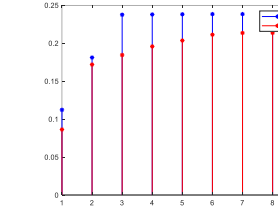
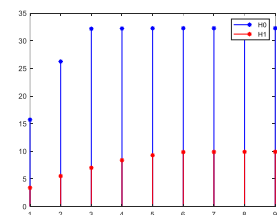
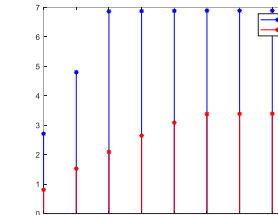
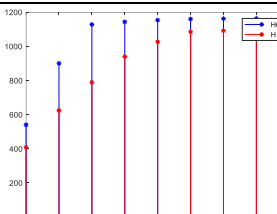
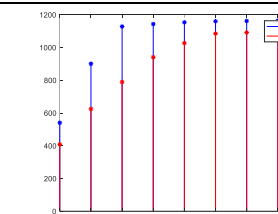
Supplementary Explanations of the Graph Signal Configuration and Its Selection

Abstract: This supplementary material primarily elucidates and verifies, through simulations, certain conditions in the proof of the effectiveness of the combination of graph signals proposed in the main text of this algorithm.

1. Majorization of the four candidate graph signal configurations.

The relationships between the mean and variance vectors of the graph signals on the strong product graphs among the four configurations of the graph signals are listed in the table below. The red dots in the figures denote the means or variances of the strong graph product signals under the null hypothesis, while the blue dot represents those under the alternative hypothesis. For the four schemes, the third and the fourth columns represent the majorization ordering of the means and the variances of the graph signals under two different hypotheses respectively, measured by the partial sum. For a specific graph signal, obtained by transforming the power spectrum or the autocorrelation function of the original signal, at an appropriate SNR, the majorization between the graph signals in a single trial under the two hypotheses matches the majorization between their means. Evidently, only schemes A and B satisfy the constraint defined in (33), that is, $\mathbf{z}_0 \prec_w \mathbf{z}_1$.

Table S1. Configurations of the graph signals on the strong product graph (SNR = -2 dB).

Scheme	Graph Signal on G_1 and G_2	The means of the graph signals on the strong product graphs under two hypotheses	The variances of the graph signals on the strong product graphs under the two hypotheses
A	$\mathbf{x}^{VPV}, \mathbf{y}^{SQIS}$	 $\mu_{A,0} \prec_w \mu_{A,1}$	 $\sigma_{A,0}^2 \prec_w \sigma_{A,1}^2$
B	$\mathbf{x}^{VPV}, \mathbf{y}^{VPV}$	 $\mu_{B,0} \prec \mu_{B,1}, \mu_{B,0} \approx \mu_{B,1}$	 $\sigma_{B,0}^2 \prec_w \sigma_{B,1}^2, \sigma_{B,0}^2 \approx_w \sigma_{B,1}^2$
C	$\mathbf{x}^{SQIS}, \mathbf{y}^{SQIS}$	 $\mu_{C,1} \prec_w \mu_{C,0}$	 $\sigma_{C,1}^2 \prec_w \sigma_{C,0}^2$
D	$\mathbf{x}^{SQIS}, \mathbf{y}^{VPV}$	 $\mu_{D,1} \prec_w \mu_{D,0}$	 $\sigma_{D,1}^2 \prec_w \sigma_{D,0}^2$

We can summarize the relationships in Table 1 as follows:

$$\begin{cases} \mu_{A,0} \prec_W \mu_{A,1}, \sigma_{A,0}^2 \prec_W \sigma_{A,1}^2, \mu_{B,0} \prec \mu_{B,1}, \mu_{B,0} \approx \mu_{B,1}, \sigma_{B,0}^2 \prec_W \sigma_{B,1}^2, \sigma_{B,0}^2 \approx_W \sigma_{B,1}^2, \\ \mu_{B,0} \prec_W \mu_{A,0}, \mu_{B,1} \prec_W \mu_{A,1}, \sigma_{B,0}^2 \prec_W \sigma_{A,0}^2, \sigma_{B,1}^2 \prec_W \sigma_{A,1}^2. \end{cases}$$

Those relationships help to explain the choice of scheme A regarding the graphs' signal configuration.

2. Detailed proofs combination of the simulation checking of the critical assuming.

1) Proposition 3: Let $p_i = \mu_{z_i} / s_i, q_i = \mu_{z_i} / s_0, E[\phi_\lambda(\mathbf{z}_\delta)] = E(\mathbf{z}_\delta^T \mathbf{L}_\lambda \mathbf{z}_\delta), \delta, \lambda = 0, 1, \mu_{z_i} = p_i s_1, \mu_{z_i} = q_i s_0, i = 1, \dots, N, \sum_{i=1}^k p_i \geq \sum_{i=1}^k q_i$, and $\Delta s = s_1 - s_0$ for $N > 2, k \leq N/2$. If $t = N \sum_{i=1}^k p_i^2 > 1, \sigma_0^2 \prec_W \sigma_1^2$ and $\Delta s \geq ths = [(\sqrt{t} - \sqrt{t-1}) / \sqrt{t-1}] s_0$, then $E[\phi_0(\mathbf{z}_0)] \leq E[\phi_1(\mathbf{z}_1)]$.

Proof: Let d_i^1 and \mathfrak{E}_1 be the degree of the i -th vertex and the vertex set on the strong product graph under H_1 . We first verify

$$E[\phi_1(\mathbf{z}_1)] - E[\phi_0(\mathbf{z}_0)] = \underbrace{\sum_{i=1}^N d_i^1 (\sigma_{1,i}^2 - \sigma_{0,i}^2)}_{I_1} + \frac{1}{2} \left[\underbrace{\sum_{(i,j) \in \mathfrak{E}_1} (\mu_{1,i} - \mu_{1,j})^2}_{I_2} - \sum_{(i,j) \in \mathfrak{E}_1} (\mu_{0,i} - \mu_{0,j})^2 \right], \quad (1)$$

Since the two functions in I_1 are both increasing Schur-convex functions from Lemma 2, and $\sigma_0^2 \prec_W \sigma_1^2$, the term $I_1 \geq 0$. For I_2 , according to Lemma 3, we have

$$\begin{aligned} N \sum_{i=1}^N (\mu_{z_i}^2 - \mu_{z_i}^2) - (s_1^2 - s_0^2) &= (N \sum_{i=1}^N p_i^2 - 1) s_1^2 - (N \sum_{i=1}^N q_i^2 - 1) s_0^2 \\ &> (N \sum_{i=1}^k p_i^2 - 1) s_1^2 - N \sum_{i=1}^k q_i^2 s_0^2 > (N \sum_{i=1}^k p_i^2 - 1) s_1^2 - N \sum_{i=1}^k p_i^2 s_0^2 \\ &= \left[\sqrt{(N \sum_{i=1}^k p_i^2 - 1)(s_0 + \Delta s)} - \sqrt{N \sum_{i=1}^k p_i^2 s_0} \right] \left[\sqrt{(N \sum_{i=1}^k p_i^2 - 1)(s_0 + \Delta s)} + \sqrt{N \sum_{i=1}^k p_i^2 s_0} \right] \end{aligned} \quad (2)$$

Clearly, if $\Delta s \geq ths$, the above equation is greater than 0, implying $E[\phi_0(\mathbf{z}_0)] \leq E[\phi_1(\mathbf{z}_1)]$. Our simulations revealed that if the SNR is greater than -9 dB, the condition $\Delta s \geq ths$ is satisfied. Further, we found that if the SNR is > -9 dB and $k \geq 1$, the condition $\Delta s \geq ths$ is satisfied, as shown in Fig. S1.

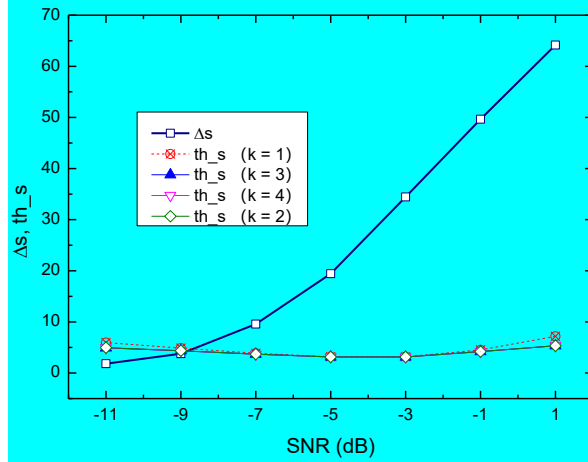


Fig. S1. Verification of $\Delta s \geq ths$ under different SNRs.

Next, we evaluate

$$\begin{aligned} E[\phi_1(\mathbf{z}_0)] - E[\phi_0(\mathbf{z}_0)] &= \sum_{i=1}^N \sigma_{0,i}^2 (d_i^1 - d_i^0) + \frac{1}{2} \left[\sum_{(i,j) \in \mathfrak{E}_1} (\mu_{0,i} - \mu_{0,j})^2 - \sum_{(i,j) \in \mathfrak{E}_0} (\mu_{0,i} - \mu_{0,j})^2 \right]. \end{aligned} \quad (3)$$

The first term of (29) is greater than 0 since $d_i^0 \leq d_i^1 = N - 1$ and the second term

$$\sum_{(i,j) \in \mathfrak{E}_1} (\mu_{0,i} - \mu_{0,j})^2 - \sum_{(i,j) \in \mathfrak{E}_0} (\mu_{0,i} - \mu_{0,j})^2 = \sum_{(i,j) \in \mathfrak{E}_0} (\mu_{0,i} - \mu_{0,j})^2 \geq 0. \quad (4)$$

Consequently, $E[\phi_0(\mathbf{z}_0)] \leq E[\phi_1(\mathbf{z}_0)]$. In summary, it follows that $E[\phi_0(\mathbf{z}_0)] \leq E[\phi_1(\mathbf{z}_0)] \leq E[\phi_1(\mathbf{z}_1)]$. ■

2) Effect of the graph signal configuration

In Section III.B, we present two schemes for defining graph signal: the VPV is defined as the graph signal for the BSPS-generated graph, and the SQIS is defined as the graph signal for the ACF-generated graph. Next, the theoretical analysis auxiliary with simulation is used further to explain the selection of the signal configuration. The signal configuration selection can be formulated as a solution for the optimization problem

$$\arg \max_{\Theta} \{df[\phi(\mathbf{z}_0), \phi(\mathbf{z}_1)]\} \quad (5)$$

$st. \mathbf{z}_0 \prec_W \mathbf{z}_1,$

where $\mathbf{z}_i = \mathbf{x}_i \otimes \mathbf{y}_i$, $i = 0, 1$, and the signal configuration set is

$$\Theta = \{(\mathbf{x}^{VPV}, \mathbf{y}^{SQIS}), (\mathbf{x}^{VPV}, \mathbf{y}^{VPV}), (\mathbf{x}^{SQIS}, \mathbf{y}^{SQIS}), (\mathbf{x}^{SQIS}, \mathbf{y}^{VPV})\}. \quad (6)$$

Let $\mathbf{z}_0 = (z_{0,i})_{N \times 1}, \mathbf{z}_1 = (z_{1,i})_{N \times 1}$ respectively be the dual independent graph signals on the strong product graphs under the null and alternative hypotheses, and $\boldsymbol{\mu}_0, \boldsymbol{\mu}_1, \boldsymbol{\sigma}_0^2, \boldsymbol{\sigma}_1^2$ be the mean and variance vectors of the graph signals $\mathbf{z}_0, \mathbf{z}_1$ respectively. Considering (24), the deflection coefficient can be further written as

$$df[\phi(\mathbf{z}_0), \phi(\mathbf{z}_1)] = \frac{\left\{ \sum_{i=1}^N (d_{0,i} \sigma_{0,i}^2 - d_{1,i} \sigma_{1,i}^2) + \frac{1}{2} \left[\sum_{(i,j) \in \mathfrak{E}_0} (\mu_{0,i} - \mu_{0,j})^2 - \sum_{(i,j) \in \mathfrak{E}_1} (\mu_{1,i} - \mu_{1,j})^2 \right] \right\}^2}{\text{Var}[\phi_0(\mathbf{z})]}, \quad (7)$$

where $d_{0,i}, d_{1,i}, i = 1, \dots, N$ represents the degrees of each vertex of graphs G_0 and G_1 , respectively. By simulation, it can be easily verified that the combination $(\mathbf{x}^{SQIS}, \mathbf{y}^{SQIS}), (\mathbf{x}^{SQIS}, \mathbf{y}^{VPV})$ cannot meet the constraint condition in (33), while we have $\mathbf{z}_{A,0} \prec_W \mathbf{z}_{A,1}, \mathbf{z}_{B,0} \prec_W \mathbf{z}_{B,1}$, as can be seen in the supplementary material. Hence, the optimization problem defined in (33) can be reduced to

$$\arg \max_{\Theta \in \Theta_0} \{df[\phi(\mathbf{z}_0), \phi(\mathbf{z}_1)]\}. \quad (8)$$

where $\Theta_0 = \{(\mathbf{x}^{VPV}, \mathbf{y}^{SQIS}), (\mathbf{x}^{VPV}, \mathbf{y}^{VPV})\}$.

Let $\mathbf{z}_{A,i} = \mathbf{x}_i^{VPV} \otimes \mathbf{y}_i^{SQIS}, \mathbf{z}_{B,i} = \mathbf{x}_i^{VPV} \otimes \mathbf{y}_i^{VPV}, i = 0, 1$. If

$$r_E = \frac{(E[\phi(\mathbf{z}_{A,1})] - E[\phi(\mathbf{z}_{A,0})])^2}{(E[\phi(\mathbf{z}_{B,1})] - E[\phi(\mathbf{z}_{B,0})])^2} \geq r_V = \frac{\text{Var}[\phi(\mathbf{z}_{A,0})]}{\text{Var}[\phi(\mathbf{z}_{B,0})]}, \quad (9)$$

then $df[\phi(\mathbf{z}_{A,0}), \phi(\mathbf{z}_{A,1})] > df[\phi(\mathbf{z}_{B,0}), \phi(\mathbf{z}_{B,1})]$. Unfortunately, it is difficult to derive r_V as the function of the statistic of the graphs signals analytically since $\text{Var}[\phi_0(\mathbf{z})]$ cannot be further simplified without any other additional conditions. As evident from Fig. S2, if $(\mathbf{x}^{VPV}, \mathbf{y}^{SQIS})$ combination is selected, $r_E \gg r_V$ holds under different SNRs in the simulations.

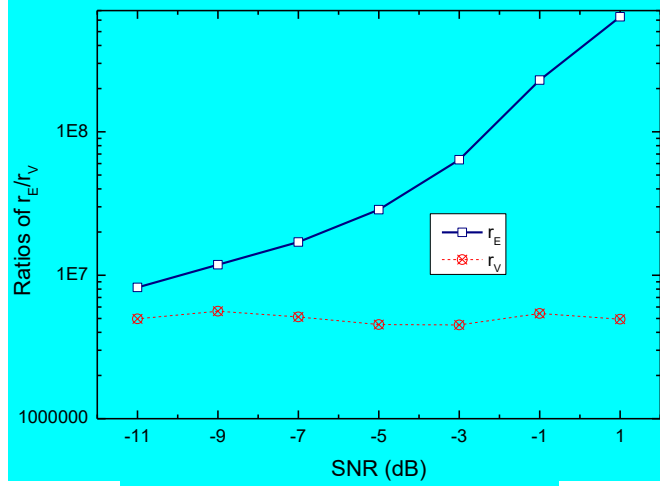


Fig. S2. Verification for the ratio $r_E \gg r_V$.

However,

$$E[\phi(\mathbf{z}_{A,1})] - E[\phi(\mathbf{z}_{A,0})] > E[\phi(\mathbf{z}_{B,1})] - E[\phi(\mathbf{z}_{B,0})] \quad (10)$$

is a necessary condition for establishing (37). From (24), it yields that

$$\begin{aligned} & \{E[\phi(\mathbf{z}_{A,1})] - E[\phi(\mathbf{z}_{A,0})]\} - \{E[\phi(\mathbf{z}_{B,1})] - E[\phi(\mathbf{z}_{B,0})]\} \\ &= \underbrace{\sum_{i=1}^N [d_{1,i}^A (\sigma_{1,i}^A)^2 - d_{0,i}^A (\sigma_{0,i}^A)^2] - \sum_{i=1}^N [d_{1,i}^B (\sigma_{1,i}^B)^2 - d_{0,i}^B (\sigma_{0,i}^B)^2]}_{I_1} + \underbrace{\frac{1}{2} \left[\sum_{(i,j) \in \mathfrak{E}_1} (\mu_{1,i}^A - \mu_{1,j}^A)^2 - \sum_{(i,j) \in \mathfrak{E}_0} (\mu_{0,i}^A - \mu_{0,j}^A)^2 \right] - \frac{1}{2} \left[\sum_{(i,j) \in \mathfrak{E}_1} (\mu_{1,i}^B - \mu_{1,j}^B)^2 - \sum_{(i,j) \in \mathfrak{E}_0} (\mu_{0,i}^B - \mu_{0,j}^B)^2 \right]}_{I_2}, \end{aligned} \quad (11)$$

where $\mathfrak{E}_i, i = 1, 0$ denotes the edge of the graph $G_i, i = 1, 0$, as shown in Figs. 3 and 4. For the first term in (40), we have

$$I_1 > (N-1) \left\{ \underbrace{\sum_{i=1}^N [(\sigma_{1,i}^A)^2 - (\sigma_{0,i}^A)^2]}_{\Delta\sigma_{10}^A} - \underbrace{\sum_{i=1}^N [(\sigma_{1,i}^B)^2 - (\sigma_{0,i}^B)^2]}_{\Delta\sigma_{10}^B} \right\}. \quad (12)$$

If $\Delta\sigma_{10}^A > \Delta\sigma_{10}^B$, (40) is greater than 0. According to Lemma 2, since $\sigma_{A,0}^2 \prec_W \sigma_{A,1}^2$ and $\sigma_{B,0}^2 \prec_W \sigma_{B,1}^2$, $\Delta\sigma_{10}^A \geq 0$ and $\Delta\sigma_{10}^B \geq 0$. Considering the elements of $\sigma_{B,0}^2 \approx \sigma_{B,1}^2 \ll 1$, $\sigma_{A,0}^2 \gg 1$ and $\sigma_{A,1}^2 \gg 1$. Hence, $I_1 \geq 0$ is easily defended. Fig. S3 shows the results of the simulations of $\Delta\sigma_{10}^A$, $\Delta\sigma_{10}^B$ at an SNR varying from -11 dB to 1 dB at steps of 2 dB. Evidently, $\Delta\sigma_{10}^A \gg \Delta\sigma_{10}^B$ can be deduced under all SNRs.

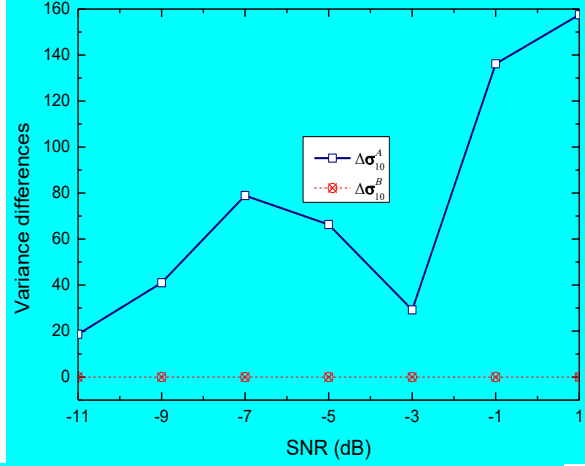


Fig. S3. Simulation results corresponding to $\Delta\sigma_{10}^A > \Delta\sigma_{10}^B$ under different SNRs

Furthermore, the term I_2 can be rewritten as

$$\begin{aligned} I_2 &= \underbrace{\sum_{(i,j) \in \mathcal{E}_1} (\mu_{1,i}^A - \mu_{1,j}^A)^2 - \sum_{(i,j) \in \mathcal{E}_1} (\mu_{0,i}^A - \mu_{0,j}^A)^2}_{\Delta_{11}(\mu_1^A, \mu_0^A)} + \underbrace{\sum_{(i,j) \in \mathcal{E}_1} (\mu_{0,i}^A - \mu_{0,j}^A)^2 - \sum_{(i,j) \in \mathcal{E}_0} (\mu_{0,i}^A - \mu_{0,j}^A)^2}_{\Delta_{10}(\mu_0^A)} \\ &\quad - \left\{ \underbrace{\sum_{(i,j) \in \mathcal{E}_1} (\mu_{1,i}^B - \mu_{1,j}^B)^2 - \sum_{(i,j) \in \mathcal{E}_1} (\mu_{0,i}^B - \mu_{0,j}^B)^2}_{\Delta_{11}(\mu_1^B, \mu_0^B)} - \underbrace{\sum_{(i,j) \in \mathcal{E}_1} (\mu_{0,i}^B - \mu_{0,j}^B)^2 - \sum_{(i,j) \in \mathcal{E}_0} (\mu_{0,i}^B - \mu_{0,j}^B)^2}_{\Delta_{10}(\mu_0^B)} \right\} \\ &= \Delta_{11}(\mu_1^A, \mu_0^A) - \Delta_{11}(\mu_1^B, \mu_0^B) + \Delta_{10}(\mu_0^A) - \Delta_{10}(\mu_0^B). \end{aligned} \quad (13)$$

Proposition 4: Let $\hat{\mu}_1^A = (\hat{\mu}_{1,i}^A)_{N \times 1}$, where

$$\hat{\mu}_{1,i}^A = \begin{cases} \mu_{1,1}^A - 1/N, & i = 1, \\ \mu_{1,i}^A, & i \neq 1, \end{cases}$$

$$\hat{s}_j = \sum_{i=1}^N \mu_{1,i}^A, i = 0, 1, \hat{s}_1 = \sum_{i=1}^N \hat{\mu}_{1,i}^A, \hat{p}_i = \hat{\mu}_{1,i}^A / \hat{s}_1, \hat{q}_i = \mu_{0,i}^A / \hat{s}_0, \Delta s_{10} = \hat{s}_1 - \hat{s}_0, \quad \text{and} \quad \sum_{i=1}^k \hat{p}_i \geq \sum_{i=1}^k \hat{q}_i, i = 1, \dots, N, \quad \text{for}$$

$N > 2, k \leq N/2$. If $\hat{t} = N \sum_{i=1}^k \hat{p}_i^2 > 1$, $\hat{\mu}_{1,1}^A > N$ and $\Delta \hat{s} \geq T_h = [(\sqrt{\hat{t}} - \sqrt{\hat{t} - 1}) / \sqrt{\hat{t} - 1}] \hat{s}_0$, then

$$\Delta_{11}(\mu_1^A, \mu_0^A) > \Delta_{11}(\mu_1^B, \mu_0^B).$$

Proof: Considering $\sum_{(i,j) \in \mathcal{E}_1} (\mu_{1,i}^B - \mu_{1,j}^B)^2$ is the Schur convex function according to Lemma 1, it yields

$$\begin{aligned} \Delta_{11}(\mu_1^B, \mu_0^B) &= \frac{1}{2} \sum_{(i,j) \in \mathcal{E}_1} [(\mu_{1,i}^B - \mu_{1,j}^B)^2 - (\mu_{0,i}^B - \mu_{0,j}^B)^2] \\ &\leq \Delta_{11}(\mu_1^{\max}, \mu_0^{\min}) = (N-1), \end{aligned} \quad (14)$$

where $\mu_0^{\min} = (1/N, 1/N, \dots, 1/N)^T \prec \mu_i^B \prec \mu_1^{\max} = (1, 0, \dots, 0)^T, i = 0, 1$. According to Lemma 3, it follows that

$$\Delta_{11}(\mu_1^A, \mu_0^A) = N \sum_{i=1}^N [(\mu_{1,i}^A)^2 - (\mu_{0,i}^A)^2] - (\hat{s}_1^2 - \hat{s}_0^2). \quad (15)$$

Further considering

$$\begin{aligned} N \sum_{i=1}^N [(\mu_{1,i}^A)^2 - (\mu_{0,i}^A)^2] - (\hat{s}_1^2 - \hat{s}_0^2) &\geq N \sum_{i=1}^N [(\mu_{1,i}^A)^2 - (\mu_{0,i}^A)^2 - 1] - (\hat{s}_1^2 - \hat{s}_0^2) \\ &\geq N \sum_{i=1}^N [(\hat{\mu}_{1,i}^A)^2 - (\mu_{0,i}^A)^2] - [(\hat{s}_1 - 1/N)^2 - \hat{s}_0^2] + 2\hat{s}_1 / N - 1 / N > N \sum_{i=1}^N [(\hat{\mu}_{1,i}^A)^2 - (\mu_{0,i}^A)^2] - [(\hat{s}_1^2 - \hat{s}_0^2)]. \end{aligned} \quad (16)$$

In the last line of (45), considering $\hat{s}_1 \gg 1/2N$, it follows that $2\hat{s}_1/N - 1/N^2 = (2\hat{s}_1N - 1)/N^2 \geq 0$. Similar to Proposition 3, if $\Delta s_{10} \geq T_h = [(\sqrt{t} - \sqrt{t-1})/\sqrt{t-1}]\hat{s}_0$, (45) is greater than 0, that is, $\Delta_{11}(\mu_1^A, \mu_0^A) \geq (N-1) \geq \Delta_{11}(\mu_1^B, \mu_0^B)$. ■

The condition $\Delta s_{10} \geq T_h$ can be verified via simulations, as depicted in Fig. S4.

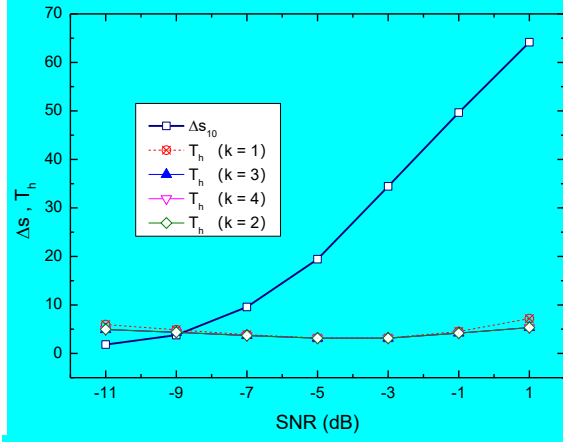


Fig. S4. Verification of $\Delta s_{10} \geq T_h$ under different SNRs.

Proposition 5: Let

$$\begin{cases} \mu_0^A = (\mu_{0,0}^A, \dots, \mu_{0,P}^A, \mu_{0,P+1}^A, \dots, \mu_{0,P}^A)^T \in \mathbb{D}_+ \\ \mu_0^B = (\mu_{0,0}^B, \dots, \mu_{0,P}^B, \mu_{0,P+1}^B, \dots, \mu_{0,P}^B)^T \in \mathbb{D}_+ \end{cases},$$

$\Delta \mu_0 = \mu_0^A - \mu_0^B = (\Delta \mu_1, \dots, \Delta \mu_P, \Delta \mu_{P+1}, \dots, \Delta \mu_{P+Q})^T$, $S_P = \sum_{i=1}^P \Delta \mu_i$, and $S_Q = \sum_{i=P+1}^N \Delta \mu_i$, where P and Q denote the number of rows and columns of the matrix $\Delta A = A_1 - A_0 = \mathbf{1}_{P \times Q}$ and $P+Q=N$. If $(QS_P - PS_Q) > 0$, then $\Delta_{10}(\mu_0^A) - \Delta_{10}(\mu_0^B) \geq 0$.

Proof: Considering

$$\begin{aligned} \Delta_{10}(\mu_0^A) - \Delta_{10}(\mu_0^B) &= \sum_{i=1}^P \sum_{j=P+1}^N (\Delta \mu_i - \Delta \mu_j) [(\mu_{0,i}^A - \mu_{0,j}^A) + (\mu_{0,i}^B - \mu_{0,j}^B)] \\ &> \sum_{i=1}^P (\mu_{0,i}^A - \mu_{0,P+1}^A) \sum_{j=P+1}^N (\Delta \mu_i - \Delta \mu_j) = \sum_{i=1}^P (\mu_{0,i}^A - \mu_{0,P+1}^A) (Q \Delta \mu_i - S_Q) > (\mu_{0,P}^A - \mu_{0,P+1}^A) (QS_P - PS_Q), \end{aligned} \quad (17)$$

since $\mu_0^A \in \mathbb{D}_+$, it follows that $(\mu_{0,P}^A - \mu_{0,P+1}^A) > 0$. If $QS_P - PS_Q > 0$, then $\Delta_{10}(\mu_0^A) - \Delta_{10}(\mu_0^B) \geq 0$. ■

Generally, as $\mu_0^A \gg \mu_0^B$, $(QS_P - PS_Q) > 0$ is easily satisfied. As evident from Fig. S5, $QS_P - PS_Q > 0$ holds under each SNR.

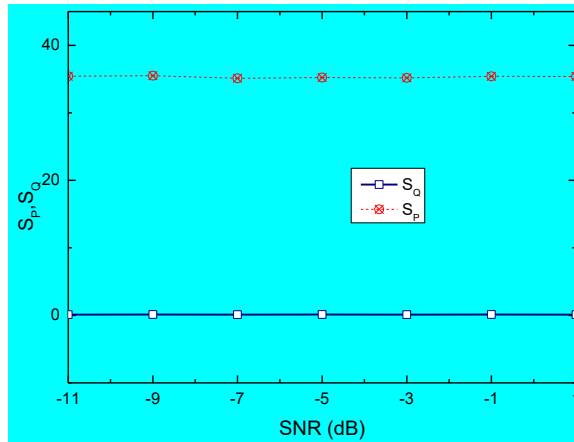


Fig. S5. Verification of the condition $(QS_P - PS_Q) > 0$.